Time-Resolved Dynamic Light Scattering Study on the Dynamics of Silica Gels during Gelation Process

Tomohisa Norisuye, Masao Inoue, and Mitsuhiro Shibayama*

Department of Polymer Science and Engineering, Kyoto Institute of Technology, Matsugasaki, Sakyo-ku, Kyoto 606-8585, Japan

Ryo Tamaki and Yoshiki Chujo

Department of Polymer Chemistry, Graduate School of Engineering, Kyoto University, Yoshida, Sakyo-ku, Kyoto 606-8501, Japan

Received August 31, 1999; Revised Manuscript Received November 10, 1999

ABSTRACT: The dynamics and structure have been compared for two types of silica gels prepared from tetramethoxysilane in dimethylformamide under acidic and basic conditions. An in-situ time-resolved dynamic light scattering (TRDLS) technique was employed to investigate the changes of the dynamics during gelation process. In both cases, a clear power-law behavior in the time−intensity correlation function, $g^{(2)}(\tau) - 1 \sim \tau^{n-1}$, was observed at the gelation threshold, from which the critical exponent of viscoelasticity, n, was evaluated. The gelation of the acid system was slower, and the gelation time was a weak decreasing function of the initial monomer concentration, C. The resultant gel was found to be made of long polysiloxane chains slightly connected with each other, which was characterized by $n \approx 0.5$. On the other hand, the gelation time of silica gels prepared with a basic catalyst was strongly dependent on C. The evaluated value $n \approx 0.73$ indicates the presence of highly branched clusters with short strands. It is demonstrated that the TRDLS technique is a powerful tool to investigate gelation process of silica from both dynamic and structural points of view.

Introduction

In the previous paper,[1] we reported that the gelation kinetics of silica−organic polymer hybrids can be quantitatively analyzed with time-resolved dynamic light scattering (TRDLS). For example, successive acquisition of time−intensity correlation functions (ICF) every 500 s allowed us to monitor precisely the change of the dynamics of a gel-forming liquid as a function of reaction time, t. The relaxation time increases with t and diverges at the gelation threshold, $t = t_{th}$. At the same time, a nonergodic effect appears just after gelation, which leads to significant suppression of the initial amplitude of ICF. Appearance of a power-law behavior in ICF at the gelation threshold is now well-known as reported by Martin et al.,[2−4] Ren and Sorensen,[5,6] and Shibayama and co-workers.[1,7]

In this paper, we focus on the time evolution of chain dynamics in gelation process of tetramethoxysilane (TMOS) prepared with two type of catalysts, i.e., acidic and basic catalysts. It will be demonstrated that TRDLS is a powerful means to determine the gelation threshold and to investigate the gelation kinetics as well as the structure of resultant gels.

Theoretical Background

Time−Intensity Correlation Function for a Gelling System. Martin et al.[3,4] reported that the time−intensity correlation function (ICF), $g^{(2)}(\tau) - 1$, at the gelation threshold is given by a sum of two contributions, i.e., a diffusive mode and a power-law behavior, as follows:

$$g^{(2)}(\tau) - 1 = \sigma_1^2\{A \exp(-\tau/\tau_f) + (1 - A)[1 + (\tau/\tau^*)]^{(n-1)/2}\}^2 \quad (1)$$

where σ_1^2 is the initial amplitude of ICF, and τ_f and τ^* are the characteristic decay time of the fast (diffusive) mode and the lower cutoff of the power-law behavior. The fast mode corresponds to the cooperative diffusion of local motions as often found in gels (the gel mode).[8] n is the critical exponent for viscoelasticity as will be discussed in section 2.2. A ($0 \le A \le 1$) is the relative strength of the diffusive mode. On the other hand, ICF for pregel solutions is given by a combination of single and stretched exponential functions, i.e.,

$$g^{(2)}(\tau) - 1 = \sigma_I^2\{A \exp(-\tau/\tau_f) + (1 - A) \times \exp[-(\tau/\tau_s)^\beta]\}^2 \quad (2)$$

where τ_f and τ_s are the characteristic relaxation times of the fast and slow modes, respectively. The slow mode in eq 2 seems to be analogous to the α-relaxation as observed in glass forming materials above the glass transition temperature. At the gelation threshold, a crossover takes place from stretched exponential to a power-law behavior.[3,6,7]

The amplitude of ICF, σ_I^2, is close to the instrumental coherence factor (usually ≈1) as far as the system is in the sol state. After gelation threshold, however, the system becomes nonergodic.[9] According to Joosten et al., σ_I^2 is given by[10]

$$\sigma_I^2 \equiv \frac{\langle I^2(0)\rangle_T}{\langle I(0)\rangle_T^2} - 1 = X(2 - X) \quad (3)$$

* To whom correspondence should be addressed.

10.1021/ma991496b CCC: $19.00
Published on Web 01/18/2000

where $\langle ... \rangle_T$ denotes time average and X is the ratio of the scattered intensity of the time-fluctuating component $\langle I_F \rangle_T$ with respect to the total intensity at a given position in a gel, $\langle I \rangle_T$, i.e.,

$$X \equiv \frac{\langle I_F \rangle_T}{\langle I \rangle_T} \quad (\text{for } A \approx 1) \tag{4}$$

The value of X decreases from unity by entering the gel state, resulting in a decrease in σ_I^2 from unity.[1]

Physical Meaning of the Critical Exponent *n*. The critical exponent, n, has the same physical origin as the power-law behavior[11,12] in the viscoelastic behavior at the gelation threshold, i.e., equivalence between the storage (G') and loss moduli (G'') as a function of angular frequency ω, i.e.,

$$G' = G'' \sim \omega^n \quad (\text{at the gelation threshold}) \tag{5}$$

The relation given by eq 5 was first reported by Winter et al.[13] Muthukumar discussed the value of n in relation to several kinds of screening effects, such as excluded-volume and hydrodynamic screening effects. By taking account of hydrodynamic screening effects, Muthukumar[14] and Martin et al.[15] derived the relation between n and the fractal dimension D,

$$n = \frac{d}{D+2} \quad (\text{without screening effect}) \tag{6}$$

where d is the space dimension (=3). By substituting $D = 2$, n is readily obtained to be $^3/_4$. In the case of percolated clusters, $D = 2.52$ leads to $n = {}^2/_3$. In the case when the excluded-volume effect is screened, D should be replaced by $\bar{D}$ as discussed by Muthukumar,[14] i.e.,

$$n = \frac{d}{\bar{D}+2} = \frac{d(d+2-2D)}{2(d+2-D)} \tag{7}$$

The validity of eq 7 for polymer gels was also discussed by Muthukumar.[16] Hence, n becomes $^1/_2$ when $D = 2$. This is the exponent that Winter et al.[13] observed in their viscoelastic measurements for poly(dimethylsiloxane) in a polymerization reactor batch. Hence, it is now well-known that the value of n is a sensitive measure of the degree of branching in a gel.[4,17]

Experimental Section

Samples. Tetramethoxysilane (TMOS), purchased from Tokyo Kasei Kogyo Co., Ltd., was purified by distillation under nitrogen. The samples for TRDLS measurements were prepared as follows: Prescribed amounts of TMOS were dissolved in 9 mL of dimethylformamide (DMF) in a 10 mm diameter test tube at room temperature under N_2 purge. Polymerization/gelation of TMOS was initiated by adding 0.24 mL of 0.1 N HCl (acidic catalyst) or 0.28 mL of 2.9 N NH_3 aqueous solution (basic catalyst) just before TRDLS measurements. The amount of water in the catalyst solutions was chosen to be stoichiometric for hydrolysis of TMOS, i.e., 4 mol of water to 1 mol of TMOS. The catalysts were used without further purification. We did not compare effects of catalyst concentrations between the acidic and basic systems in this paper since the efficiency of the catalysts is inherently different between the two cases. Instead, the gelation time is studied as a function of the initial monomer (TMOS) concentration, C (3, 4.5, 5, and 10 wt %), at fixed catalyst concentrations.

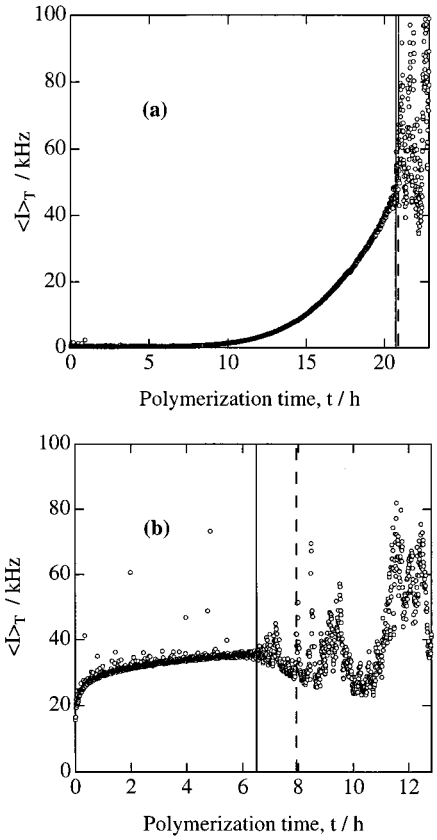

Figure 1. Scattered intensity $\langle I \rangle_T$ variations of TMOS ($C = 5$ wt %) during gelation process with (a) the acidic and (b) the basic catalysts. The solid and dashed lines indicate the time where strong fluctuations in $\langle I \rangle_T$ appeared and the time where a power-law behavior appeared in the time−intensity correlation function (ICF), respectively.

Dynamic Light Scattering. TRDLS measurements were conducted on a DLS/SLS-5000 compact goniometer (ALV, Langen, Germany) coupled with a 22 mW helium−neon laser source (Uniphase, U.S.A.). A high counting rate of the scattered intensity and a high coherence (more than 0.98) in ICF were achieved owing to employment of a set of a static and dynamic enhancers and a high-quantum efficient avalanche−photodiode detection system. The TRDLS measurements were carried out at 60 °C as a function of polymerization time, t. Scattered intensity data from the reactor batch were collected as a function of t from which ICF was calculated in a wide range of logarithmic lag time, log τ.

Results and Discussion

Determination of the Gelation Threshold. Figure 1 shows the scattered intensity variations of TMOS ($C = 5$ wt %) during gelation process with (a) the acidic and (b) the basic catalysts, where $\langle I \rangle_T$ denotes the time average scattered intensity observed at the fixed scattering angle of 90°. It is clearly seen that the two systems exhibit quite different time courses of $\langle I \rangle_T$. In the case of (a), $\langle I \rangle_T$ gradually increased for $t < 20.74$ h. This indicates that growth of poly(methoxysilane) clusters is fairly slow. However, for $t \geq 20.74$ h (marked with the solid line), strong fluctuations in $\langle I \rangle_T$ appeared, indicating an appearance of structural inhomogeneity.[18] The dashed line indicates the gelation threshold, t_{th}, determined by the appearance of a power-law behavior as will be discussed later. In this particular case, however, the difference between the two systems is negligible. On the other hand, $\langle I \rangle_T$ for the basic system increased rapidly at the very early stage of reaction, i.e.,

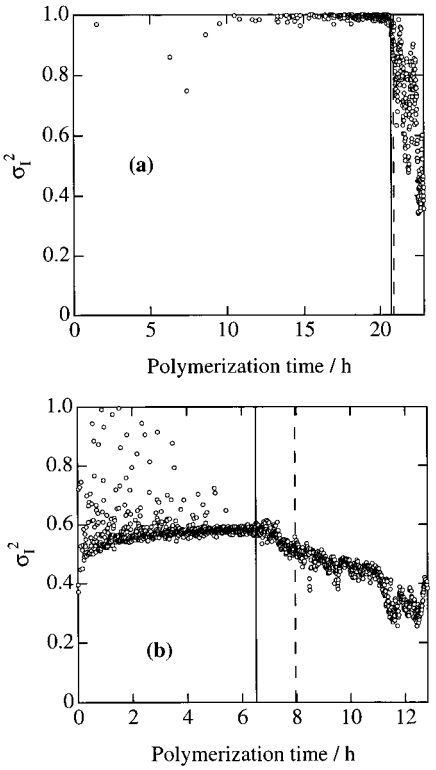

Figure 2. Variations of the initial amplitude of ICF, σ_I^2, for (a) the acidic and (b) the basic systems (C = 5 wt %). The meaning of the solid and dashed lines is the same as in Figure 1.

$t \approx 1$ h, followed by a gradual increase. The stepwise increase in $\langle I \rangle_T$ at the very beginning of polymerization indicates that glasslike rigid clusters are instantly formed at this stage and strongly scatter the incident light. Then, strong fluctuations in $\langle I \rangle_T$ appeared at 6.51 h (solid line). On the other hand, the gelation threshold was determined to be $t_{th} \approx 7.94$ h (dashed line) by subsequent power-law analysis. It is noteworthy that the difference between the two times, i.e., the time at strong fluctuations in $\langle I \rangle_T$ appearing and that at t_{th}, is quite large in the basic system. This point will be addressed later. Yamane et al.[19] observed a similar feature on pH dependence of gelation kinetics in silica gels, i.e., slow (in acidic systems) and fast gelation (in basic systems), by X-ray scattering and viscosity measurements. We demonstrated that light scattered intensity is also quite sensitive to detect the gelation threshold.

Figure 2 shows the variations of ICF, σ_I^2, for (a) the acidic and (b) the basic systems (C = 5 wt %). In the case of (a), a low statistics of the photon counting at the early stage did not provide a reliable value of σ_I^2. For $10 < t < 20$ h, σ_I^2 is close to unity, indicating that the system is ergodic. The following suppression of σ_I^2 for $t > 20.99$ h is a result of gelation (the dashed line in Figure 1a). It is rather surprising that the value of σ_I^2 for the basic system is much lower than unity (≈ 0.6) from the very beginning of polymerization. However, t_{th} is determined as a point exhibiting a power law (the dashed line in Figure 1).

It should be noted here that one has to take ensemble average of ICF instead of time average, $g^{(2)}(\tau)$, to describe a nonergodic system. The ensemble average ICF, $g_E^{(2)}(\tau)$, is given by

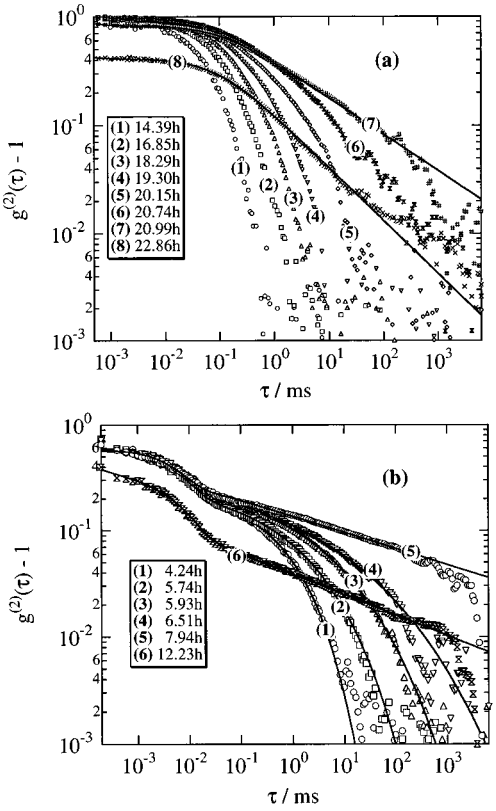

Figure 3. Double-logarithmic plots of ICFs during gelation process for (a) the acidic and (b) the basic systems (C = 5 wt %). The solid lines in (a) and (b) are the fits with eqs 1 and 2, respectively.

$$g_E^{(2)} \equiv \frac{\sum_p \langle I_p(0) \rangle_T^2 g_p^{(2)}(\tau)}{\sum_p \langle I_p(0) \rangle_T^2} \tag{8}$$

where the subscript p means that the quantity is sample-position-dependent. As a matter of fact, σ_I^2 becomes sample-position-dependent and is much less than unity for $t > t_{th}$ because $\langle I_p(0) \rangle_T$ is now position (p)-dependent. However, we disclosed the fact that the shape of $\ln[g^{(2)}(\tau) - 1]$ was quite similar to each other, and only the prefactor σ_I^2 varies with the sample position for $t > t_{th}$. Furthermore, a simultaneous measurement of $g^{(2)}(\tau)$ at many sample positions as a function of t is quite difficult. Hence, we simply evaluate $g^{(2)}(\tau)$ in this work.

Power-Law Analysis. Figure 3 shows the double-logarithmic plots of ICFs during gelation process for (a) the acidic and (b) the basic systems (C = 5 wt %). First, we discuss the ICFs for the acidic system. In the beginning ($t < 14$ h), the scattered photons are too few to build ICF. However, for $t > 14$ h, ICF shows a characteristic decay time at $\tau \approx 10^{-1}$ ms. At $t \approx 21$ h, the ICF has a long tail at the larger value of τ. At this point, the ICF seems to be well described with a power-law function, indicating $t_{th} \approx 21$ h. The solid lines on curves 7 and 8 in Figure 3a were obtained by fitting ICF with eq 1 to the case of $t = 20.99$ and $t = 22.86$ h. This fit gives $n = 0.60 \pm 0.04$. A further discussion on the exponent will be given in the next section. For $t > 20.99$ h, the value of $\sigma_I^{(2)} \equiv [g^{(2)}(\tau \rightarrow 0) - 1]$ becomes much lower than unity due to the nonergodicity of the gel.

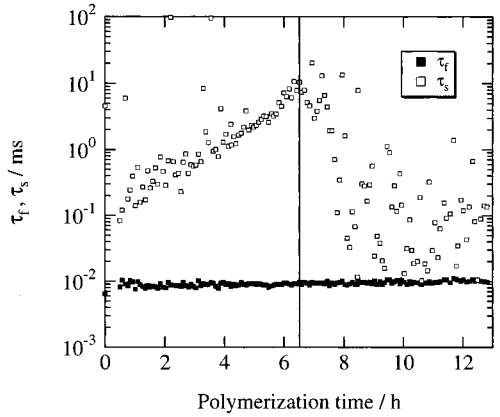

Figure 4. Time evolution of the characteristic decay times for the fast and slow modes, τ_f and τ_s, respectively.

Next, we discuss the time evolution of the ICFs for the basic systems. As shown in Figure 3b, the shapes of the ICFs are different from those of the acidic system. The solid lines are the fits with eq 2 (i.e., a stretched exponential function), which reproduce ICFs quite successfully. It should be noted that the ICFs of the acidic system were not represented by eq 2 even for $t < t_{th}$. Such a stretched exponential behavior for the slow mode in the basic system studied here is also reported by Martin et al.[3] for TMOS and by Ikkai et al.[7] for the sol state of poly(vinyl alcohol)−Congo Red complex. The common feature of the stretched exponential behavior is that the longest relaxation time, τ_s, is finite; in other words, the largest cluster is finite (a sol).

Figure 4 shows the time evolution of the characteristic decay times, τ_f and τ_s, for the basic gel (C = 5 wt %). Surprisingly, the value of τ_f does not change with t. This indicates that the fast mode (i.e., the local chain mobility) appears at the very beginning and is well preserved during the gelation process. On the other hand, τ_s increases exponentially with t. Similar phenomena were observed by Martin et al.[3,4] in a gelation process of TMOS with a basic catalyst for $t < t_{th}$, by Lin et al.[20] for many kinds of colloids, and by Shibayama and co-worker for a bulk polymerization of styrene.[21] Though τ_s starts to decrease at t = 6.51 h (indicated by the solid line), this is simply a result of gelation at which a power-law behavior appears and the stretched exponential analysis becomes invalid. However, this analysis is still useful to determine the gelation threshold. The time indicated with the solid line in Figure 1b was thus determined.

Figure 5 shows the variation of n as a function of polymerization time, t. There seems to be a significant difference in the values of n although they are scattered. For the acidic system (C = 5 wt %), the n decreases gradually from 0.6 and reaches to 0.5 as the polymerization goes on. The case n = 0.5 is the same as that obtained by Winter et al.[13] as discussed in section 2.2. Hence, it can be concluded that the gel consists of long chains slightly cross-linked with each other. On the other hand, the values of n for the basic system (C = 5 wt %) are larger than 0.7. This suggests that the gel is highly branched.

Figure 6 shows the t dependence of the stretched exponent, β, for the basic system (C = 5 wt %) obtained by curve fitting (Figure 3b). It seems that β decreases with t and reaches effectively zero at $t > t_{th}$ (≈6.6 h). This is reasonable since a power-law behavior appears

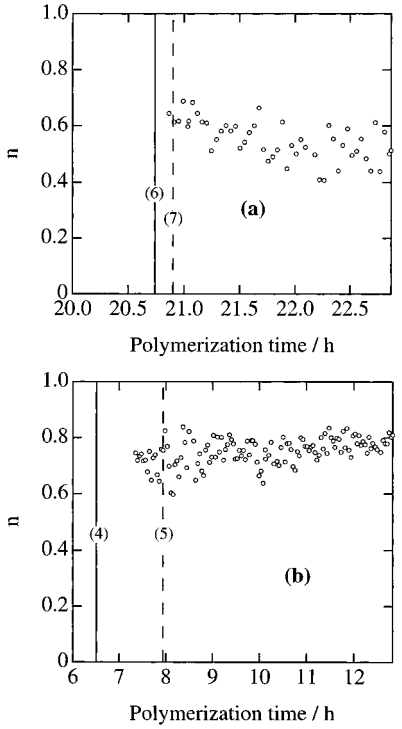

Figure 5. Variation of n as a function of polymerization time, t.

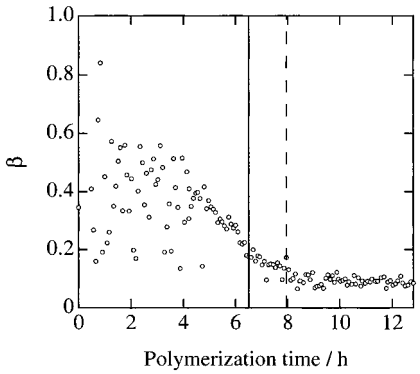

Figure 6. t dependence of the stretched exponent, β, for the basic system obtained by curve fitting with eq 2 (Figure 3b).

at $t \approx t_{th}$, and the power law corresponds to the case of $\beta = 0$.

***C* Dependence of t_{th} and Its Crossover.** In the preceding sections, it has been demonstrated that the gelation time, t_{th}, can be uniquely determined by TRDLS. Now, we apply this technique to investigate the initial monomer concentration, C, dependence of t_{th}. Figure 7 shows the variation of t_{th} with C for (a) acidic and (b) basic systems. The gelation time for the acidic system gradually decreases with increasing C. However, t_{th} is rather C independent and is estimated to be roughly 20 h. This may be due to the slow kinetics of hydrolysis (electrophilic reaction) and subsequent condensation. On the other hand, t_{th} for the basic system strongly depends on C, and t_{th} varies from hundreds of hours to a few seconds by changing C from 2% to 10%. Such a strong C dependence of t_{th} results from its characteristic reaction curve. One may assume that the reaction curve (conversion curve) has a similar t dependence to that of the intensity variation curve (Figure 1). This assumption allows the following discussion: Figure 1b suggests that the reaction rate is quite rapid in the beginning and then slows down after reaching

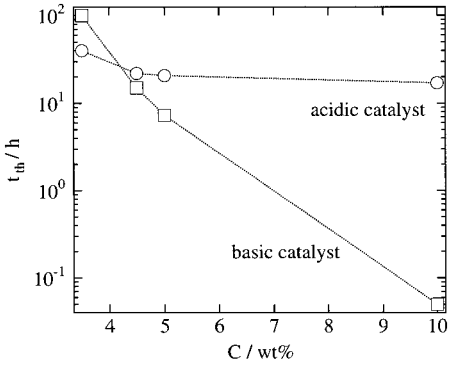

Figure 7. Variation of t_{th} with C for (a) acidic and (b) basic systems (C = 5 wt %).

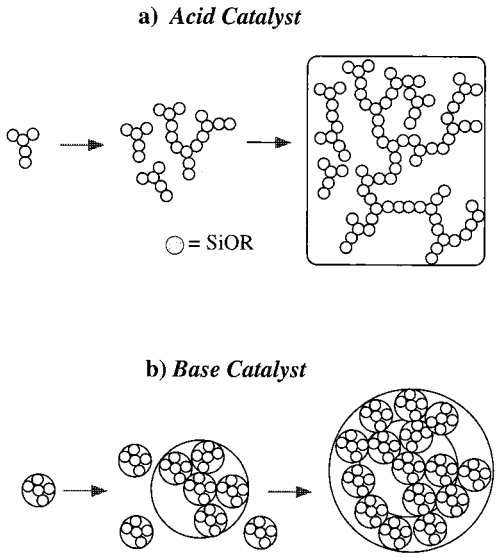

Figure 8. Schematic representation showing the gelation mechanisms for (a) acidic and (b) basic gels.

the plateau region, the so-called two-step aggregation.[4] If C is high enough, growing clusters easily overlap with each other before reaching the plateau in the reaction curve. In this case, t_{th} (the basic system) $\ll t_{th}$ (the acidic system). On the other hand, if C is low, it takes long time for the clusters to overlap, resulting in t_{th} (the basic system) $> t_{th}$ (the acidic system). In other words, the kinetics of gelation is very sensitive to C when a basic catalyst is used. Though this type of strong pH dependence in gelation kinetics was also reported by Yamane et al.,[19] such a strong C dependence of t_{th} disclosed in this study is quite surprising.

Comparison of the Gelation Mechanism. Taking account of the experimental findings disclosed above, we propose gelation schemes of TMOS. In Figure 8a is shown a growth of silica clusters that are similar to a polymerization of linear polymer chains with a small fraction of cross-links. In this case, the excluded volume effect is strongly screened by neighboring chains. This leads to $n \approx 0.5$, as observed by Winter et al.[13] and discussed in section 2.2. A basic catalyst, on the other hand, makes a TMOS monomer to be a tetrafunctional silanol group, leading to a highly branched cluster formation. In this case, n is expected to be $^3/_4$. As a matter of fact, the TRDLS measurements gave $n \approx 0.73$ in our study. Therefore, the growth of silica clusters seems to be drawn like Figure 8b. These findings disclosed in this work are in good agreement with the review by Brinker and Scherer,[22] who discussed the structure of silica gels on the basis of experimental results obtained by viscosity and small-angle X-ray scattering measurements. That is, an acid catalyst leads to chainlike (or linear) molecules, while highly branched clusters are formed by basic catalyst. However, the following fact should be stressed: The TRDLS is advantageous because it allows one to conduct a real-time observation of gelation process.

Recently, we also found a similar pH dependence of aggregation and gelation process in a biological system, i.e., β-lactoglobulin aqueous solutions.[23] In the forthcoming paper, we discuss the similarity between the two systems in more detail.

Conclusions

The gelation kinetics of TMOS was investigated by TRDLS. The following facts were disclosed: (1) The gelation kinetics is quite different between two TMOS systems prepared with acidic and basic catalysts. (2) The gelation threshold can be accurately determined by TRDLS as an appearance of a power-law behavior in ICF both gels prepared with acidic and basic catalysts. (3) The ICF is described with a stretched exponential function for the basic pregel clusters, and the stretched exponent β is reduced to zero by approaching the gelation threshold. (4) The gelation rate is strongly dependent on the initial monomer concentration, C, for the basic gels, while that of acidic gels is a weak function of C. As a result, a crossover takes place in the C dependence curve of t_{th}. (5) The values of the power-law exponent n are significantly different in the two systems; i.e., $n \approx 0.73$ for the basic gels and $n \approx 0.5$ for the acidic gels. These values indicate that acidic gels consist of long polysiloxane chain with a small fraction of cross-links, while the basic gels comprise a highly branched network.

Acknowledgment. This work is partially supported by the Ministry of Education, Science, Sports and Culture, Japan (Grant-in-Aid, 09450362, 10875199, and 11305067). Thanks are due to the Cosmetology Research Foundation, Tokyo, for financial assistance. T.N. acknowledges the Research Fellowship of the Japan Society for the Promotion of Science for Young Scientists.

References and Notes

(1) Norisuye, T.; Shibayama, M.; Tamaki, R.; Chujo, Y. *Macromolecules* **1999**, *32*, 1528.
(2) Martin, J. E.; Wilcoxon, J.; Adolf, D. *Phys. Rev. A* **1987**, *36*, 1803.
(3) Martin, J. E.; Wilcoxon, J. *Phys. Rev. Lett.* **1988**, *61*, 373.
(4) Martin, J. E.; Wilcoxon, J.; Odinek, J. *Phys. Rev. A* **1991**, *43*, 858.
(5) Ren, S. Z.; Shi, W. F.; Zhang, W. B.; Sorensen, C. M. *Phys. Rev. A* **1992**, *45*, 2416.
(6) Ren, S. Z.; Sorensen, C. M. *Phys. Rev. Lett.* **1993**, *70*, 1727.
(7) Ikkai, F.; Shibayama, M. *Phys. Rev. Lett.* **1999**, *82*, 4946.
(8) Tanaka, T.; Hocker, L. O.; Benedek, G. B. *J. Chem. Phys.* **1973**, *59*, 5151.
(9) Pusey, P. N.; van Megen, W. *Physica A* **1989**, *157*, 705.
(10) Joosten, J. G. H.; McCarthy, J. L.; Pusey, P. N. *Macromolecules* **1991**, *24*, 6690.
(11) Doi, M.; Onuki, A. *J. Phys. II* **1992**, *2*, 1631.
(12) Onuki, A. *J. Non-Cryst. Solids* **1994**, *172−174*, 1151.
(13) Winter, H. H.; Chambon, F. *J. Rheol.* **1986**, *30*, 367.
(14) Muthukumar, M. *J. Chem. Phys.* **1985**, *83*, 3161.
(15) Martin, J. E.; Adolf, D.; Wilcoxon, J. P. *Phys. Rev. A* **1989**, *39*, 1325.
(16) Muthukumar, M. *Macromolecules* **1989**, *22*, 4656.

(17) Adam, M.; Lairez, D. In *Sol−Gel Transition*; Cohen Addad, J. P., Ed.; John Wiley & Sons: New York, 1996; p 87.
(18) Shibayama, M. *Macromol. Chem. Phys.* **1998**, *199*, 1.
(19) Yamane, M.; Inoue, S.; Yasumori, A. *J. Noncryst. Solids* **1984**, *63*, 13.
(20) Lin, M. Y.; Lindsay, H. M.; Weitz, D. A.; Ball, R. C.; Klein, R.; Meakin, P. *Phys. Rev. A* **1990**, *41*, 2005.
(21) Shibayama, M.; Ozeki, S.; Norisuye, T. Manuscript in preparation.
(22) Brinker, C. J.; Scherer, G. W. *J. Non-Cryst. Solids* **1985**, *70*, 301.
(23) Takata, S.; Shibayama, M.; Tanaka, N. *Macromolecules*, manuscript in preparation.

MA991496B